

Molecular motion in melt samples of poly(propylene glycol) studied using dielectric and Kerr effect relaxation techniques

Martin S. Beevers, David A. Elliott and Graham Williams*

The Edward Davies Chemical Laboratories, The University College of Wales, Aberystwyth, Dyfed SY23 1NE, UK

(Received 19 April 1979; revised 15 June 1979)

Dielectric relaxation times and electro-optical Kerr-effect relaxation times have been measured for melt samples of pure poly(propylene glycol) of nominal molecular weight 1025, 2025 and 4000, over the temperature range 209K–255K. Kerr-effect relaxation curves were analysed in terms of two main components: a 'fast' primary process (A), associated with a negative optical birefringence; and a 'slow' secondary process (B), associated with a positive optical birefringence. Measurement of dielectric loss at different frequencies for poly(propylene glycol) of molecular weight 2025 and 4000 indicated two main relaxation processes: a 'fast' process (the normal α -process), which carried with it most of the dielectric loss; and a 'slow' secondary process of much smaller amplitude. The close correspondence between dielectric and Kerr-effect relaxation times, for the primary and secondary relaxation processes, indicated that these techniques are probing effectively different aspects of the same molecular motion. Dielectric and Kerr-effect relaxation times for the secondary process depended greatly on the molecular weight of the polymer and were compared with the predictions of the models for the reptational motions of chains in the bulk polymer, as proposed by De Gennes and by Doi and Edwards.

INTRODUCTION

The motions of flexible polymer molecules may be studied using a variety of relaxation, absorption, fluorescence and scattering techniques. Studies of bulk amorphous polymers have been made using dielectric relaxation^{1–4}, mechanical relaxation^{1,5}, n.m.r.^{6–8} and quasi-elastic neutron scattering⁹, and of polymers in solution using dielectric^{3,10}, n.m.r.^{11,12}, quasi-elastic light scattering¹³, viscoelastic⁵ and fluorescence depolarization¹⁴ techniques. The relaxation behaviour of solid polymers, bulk amorphous polymers and polymers in solution, as studied using dielectric and related techniques, have been recently reviewed^{15,16}.

The qualitative and semi-quantitative aspects of the relaxation behaviour of polymer molecules are interpreted generally in terms of the motion of an intrinsic molecular probe, the nature of which is determined by the experimental technique being employed. Examples of such probes include the dipole moment vector for dielectric relaxation, the internuclear vector for ¹³C n.m.r. relaxation and the emission transition moment for fluorescence depolarization. The rate of reorientation of the molecular probe may be readily determined experimentally as an average correlation time. However, it is difficult to establish unequivocally, for a particular relaxing system, the mechanism for the motion of the molecular probe. Many models for the motion of polymer chains have been proposed^{1,3,5,13–22} which include: (1) the rotational and translational motion of the whole chains

via small-step diffusion, normal-mode diffusion or 'reptational' diffusion, and (2) the rotational and translational motion of parts of chains via small-step diffusion or by discrete transitions within prescribed barrier systems. Relaxation data obtained from a single experimental technique may be rationalized by a variety of models for molecular motion with each model having its own adjustable parameters. However, it has been emphasized in earlier work^{23,24} that it is not possible to determine the mechanism for motion from the results of a single experimental technique since each technique yields information on only a part of the total time-dependent orientation distribution function. This limitation may be illustrated by the rotational motion of a rigid dipolar group attached to a polymer chain. The dipole moment time autocorrelation function for this process is given by (ref. 25, p. 707):

$$\begin{aligned} \langle \mu(O) \cdot \mu(t) \rangle &= \mu^2 \int f(\Omega, t/\Omega_o, 0) \cos \Theta(t) d\Omega d\Omega_o \\ &= \mu^2 \sum_K^3 \langle D_{1,K,O}(\Omega(O)) D_{1,K,O}(\Omega(t)) \rangle \end{aligned} \quad (1)$$

where $f(\Omega, t/\Omega_o, 0) d\Omega d\Omega_o$ is the conditional probability of obtaining the coordinates of the dipolar group in the solid angle $d\Omega$ around Ω at time t given that the group was oriented in the solid angle $d\Omega_o$ around Ω_o at an initial time

* To whom correspondence should be addressed

zero. Θ is the angle through which the dipole moment vector moves during the time interval t and $D_{1,K,O}$ is the appropriate element of the Wigner rotation matrix. The terms enclosed in angular brackets, in equation 1, are time-dependent correlation functions of the angular motion of the dipolar group, expressed in Euler-angle rotation. For a linear molecule the dipole moment correlation function reduces to $\mu^2 \langle P_1(\cos \Theta(t)) \rangle$, where P_n denotes the n th Legendre polynomial^{23,25}. Dielectric studies of simple molecular systems^{26,27} determine the correlation function $\langle \mu(O) \cdot \mu(t) \rangle$, but this quantity alone is not sufficient to completely define the conditional probability function $f(\Omega, t/\Omega_o, 0)$. By combining the results of complementary experiments which determine different but related time correlation functions for the motion of the molecular probe, the conditional probability function $f(\Omega, t/\Omega_o, 0)$ may be described more precisely. Two techniques which form such a complementary pair are dielectric relaxation and Kerr-effect (decay) relaxation²⁸⁻³⁰, since these depend on $\langle P_1(\cos \Theta(t)) \rangle$ and $\langle P_2(\cos \Theta(t)) \rangle$, respectively. Conclusions concerning the mechanism(s) for molecular motion are then based on all of the available relaxation data.

Studies of this kind have been carried out for simple glass-forming molecular liquids^{23,24,31,32}, in which the applicability of different models for reorientational motion was tested.

In order to clarify the mechanisms responsible for the α -relaxation in bulk amorphous polymers, the dielectric and Kerr-effect relaxation behaviour of liquid poly(propylene glycol) (PPG) was studied³³ using the above approach. Since the intrinsic Kerr constant of a low molecular weight fraction of pure PPG is quite small, dilute solutions of tri- n -butyl ammonium picrate (TBP)[†] in PPG were studied using the solute as a probe of the motions of the solvent molecules. For this system it was observed that the solute (TBP) molecules relaxed approximately 30 times more slowly than the chain-segments of the surrounding polymer molecules. Thus, although these studies determined the rates of rotational diffusion for the solute and solvent molecules, it was concluded that the solute did not act as an explicit probe of the solvent motions. As a consequence of these observations it was decided to study the relaxation behaviour of a pure sample of low molecular weight PPG ($MW \sim 1025$) using dielectric and electro-optic methods³⁴.

The unusual relaxation data obtained for this system were tentatively interpreted in terms of two main relaxation processes³³. The aim of the present study has been to extend and confirm the nature of the molecular motion in pure melt samples of poly(propylene glycol) of different molecular weight.

EXPERIMENTAL

Substantial modifications to the Kerr-effect apparatus^{23,24,32} were recently undertaken in order to improve sensitivity. The essential features of the present instrument will be briefly described.

The source of light was a Spectra-Physics 2-MW helium-neon laser (Model 138P) which has a linearly polarized output at 633 nm. Additional optical components, numbered in order of appearance after the laser were: (1) a Glan-type polarizer; (2) Kerr cell; (3) $\lambda/4$ mica retarder plate (not required for quadratic detection); (4) a Glan-type analyser

mounted on a rotatable circular scale; (5) a biconvex diffuser lens ($f = 5$ cm); (6) a 1 mm diameter pin-hole; and (7) a Mullard 56 TVP photomultiplier tube. The latter has an S20 type photocathode which has good sensitivity at 633 nm.

Linear and quadratic detection methods were employed for the recording of optical transients³⁰. For linear detection the transmission plane of the polarizer and the slow axis of the $\lambda/4$ retarder were parallel and were oriented at 45° to the direction of the applied electric field. The analyser was rotated by 5° from the position of extinction (in the absence of an applied electric field) with the sense of rotation chosen to give an increase in the intensity of light when the electric field was applied. Quadratic detection was readily achieved by removing the $\lambda/4$ retarder and rotating the analyser, in the absence of an applied electric field, to give an extinction of the light.

A Datalab Transient Recorder (DL 920), used to convert the optical transients into digital form, was connected to a Tektronix 7313 Mainframe storage oscilloscope (fitted with a dual amplifier 7A18N and a dual time base 7B53 AN), and to a Hewlett-Packard Model 7035 B X-Y plotter. This arrangement permitted optical transients to be monitored visually before plotting was initiated. The transient recorder was also interfaced to a punch tape machine (Data Dynamics 1133) which enabled data to be recorded on paper tape for subsequent analysis using a digital computer. Dielectric measurements were made concurrently on the same sample using a General Radio 1620-A Bridge Assembly with the Kerr cell connected as a two-terminal dielectric cell. This allowed a direct comparison to be made between dielectric and Kerr-effect data under as near identical conditions as possible. The temperature of the sample was controlled to within ± 0.05 K over the range 200 K–310 K using a Lauda Ultra Kryostat and methanol as the heat-exchange liquid.

Measurements of the equilibrium and dynamic Kerr-effects of poly(propylene glycol) were difficult because the intrinsic Kerr constants are small and had to be measured at low temperatures. The main problem concerned the windows of the Kerr cell which had to be maintained free of condensed water and strain birefringence. Condensation was eliminated by using double windows separated by a space filled with a stream of dry air. Paper washers were used to effect a seal between the Kerr cell and the inner windows. Each inner window was held in position by a spring-loaded steel ring. As a result, δ (strain) was estimated to be less than 400μ radian.

Rectangular-shaped high voltage pulses of duration $100 \mu\text{s}$ –60 s and amplitude 0–8 kV were generated using either a valve-powered amplifier or a high-voltage reed switch in conjunction with a Brandenburg Model 707 R power supply unit.

Low molecular weight fractions of poly(propylene glycol), supplied by BDH Chemicals Ltd., had nominal molecular weights of 1025 (PPG 1025) and 2025 (PPG 2025). Their water content was specified to be less than 0.1% by wt. A sample of poly(propylene glycol) having a molecular weight of approximately 4000 (PPG 4000) was a gift from Prof. A. J. Barlow. All the samples were dried over zeolite before use.

RESULTS

Figure 1 shows dielectric relaxation data obtained for a sample of PPG 4000 at temperatures above the glass-transition point. A small secondary (B) dispersion in addi-

[†] An ion-pair possessing a large intrinsic Kerr constant

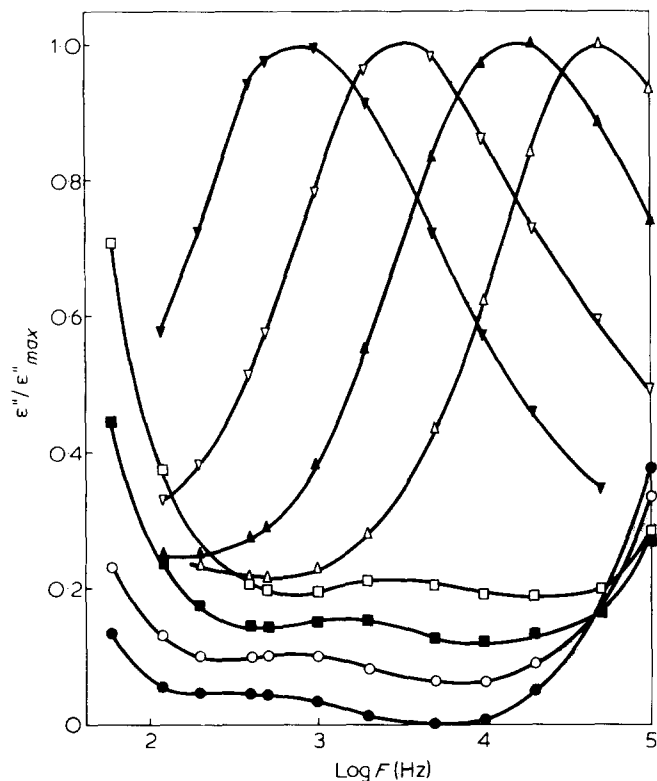


Figure 1 Normalized dielectric loss $\epsilon''/\epsilon''_{max}$ against frequency for melt samples of PPG 4000 at ∇ 220K, \triangle 224K, \blacktriangle 228K, \triangle 233K, \bullet 245K, \circ 247K, \blacksquare 251K, \square 254K. For the sake of clarity the data at 251K, 247K, 245K have been displaced downwards by 0.06, 0.12, 0.18 units of $\epsilon''/\epsilon''_{max}$, respectively

tion to the primary A-process (or α -process) is clearly evident for samples at the higher temperatures in the range studied. The frequency location of the secondary relaxation process, as a function of temperature, is similar to that observed by Baur and Stockmayer³⁵ for a sample of PPG of almost the same molecular weight. Dielectric loss curves of PPG 2025 (see refs. 34, 35) also show the presence of two relaxation processes but with a separation in frequency substantially less than that observed for PPG 4000. For melt samples of PPG 1025, a secondary dielectric dispersion could not be resolved in the presence of the primary dispersion. Dielectric loss curves for the secondary process, and the corresponding frequency of maximum dielectric loss, were derived from the total loss curves by subtracting the contributions to the loss due to d.c. conductivity and the primary process.

In Figure 2 the optical phase retardation, δ , between plane polarized components of light parallel and perpendicular to the applied electric field E is shown plotted against the square of the applied field for a sample of PPG 1025 at 226 K. Also shown in Figure 2 is the corresponding plot obtained for pure carbon tetrachloride at 298 K. The Kerr constant, B , of PPG 1025 at 226 K was calculated from the ratio of the gradients and the published Kerr constant of carbon tetrachloride³⁶ ($B_{CCl_4} = 0.88 \times 10^{-15} V^{-2} m$) and found to be $-3.1 \times 10^{-15} V^{-2} m$. Le Fèvre and Sundaram³⁷ observed negative molecular Kerr constants for poly(propylene glycol) in solution in benzene for molecular weights greater than 10^3 . Aroney and coworkers³⁸ have reported small negative infinite-dilution molecular Kerr constants ($\infty [mK_2]$) of several di- n -alkyl ethers, including di- n -propyl ether, the closest in structure to the repeat unit of PPG.

The present study is primarily concerned with measuring the time-dependent Kerr-effect of melt samples of

poly(propylene glycol) in the temperature range 212K–253K. A large number of optical transients were recorded using the quadratic method of detection. However, since the optical birefringence changes sign during the decay régime, following the step-removal of the electric field, it was often preferable to use linear detection, since this improves the signal-to-noise ratio and produces optical transient curves that are amenable to an immediate visual interpretation. Figure 3 shows optical transients obtained for PPG 1025, PPG 2025 and PPG 4000 recorded at similar temperatures using linear detection. The overall shape of the optical transient curves depends quite markedly on molecular weight, but is independent essentially of temperature (over the range studied here), provided that comparisons are made using time-normalized curves.

It is generally accepted that significant optical rise and decay transients will be obtained only if the relaxing system

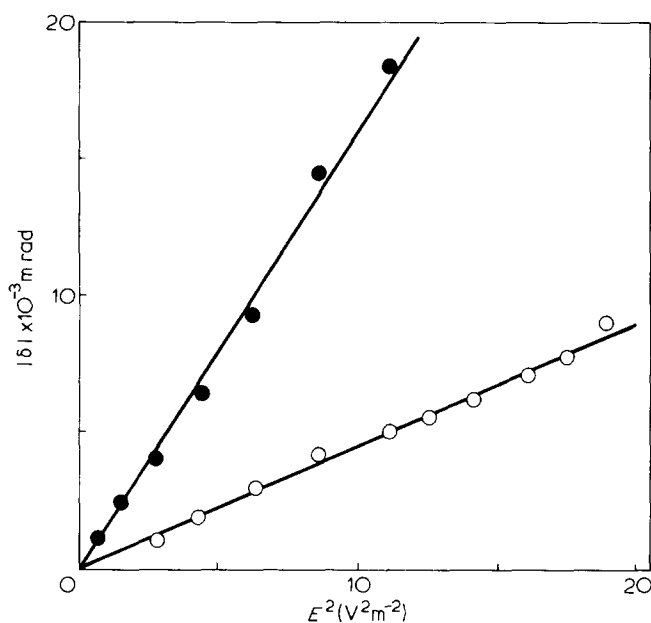


Figure 2 Optical retardation $|\delta|$ vs. square of applied electric field, E^2 , for PPG 2025 at 226K (\bullet) and carbon tetrachloride at 298K (\circ). Optical pathlength is 7.45 cm. Electrode separation is 0.114 cm

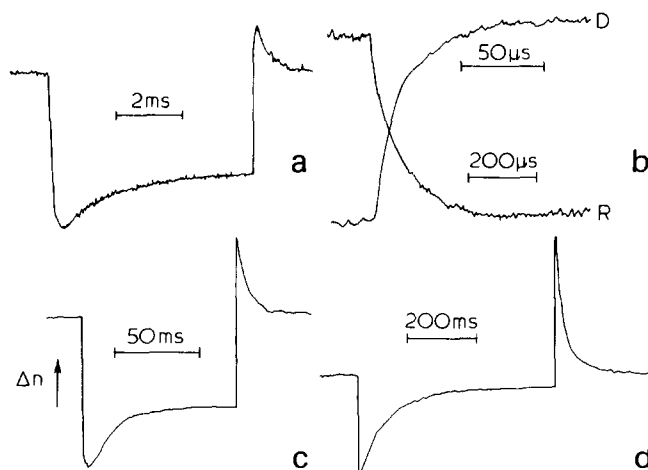


Figure 3 Linear Kerr-effect transients of melt samples of poly(propylene glycol) obtained using electric field strengths of $\sim 4 V m^{-1}$ (a) PPG 1025 at 225K, (b) Rise and decay transients of PPG 1025 at 225K, (c) PPG 2025 at 221K, (d) PPG 4000 at 224K

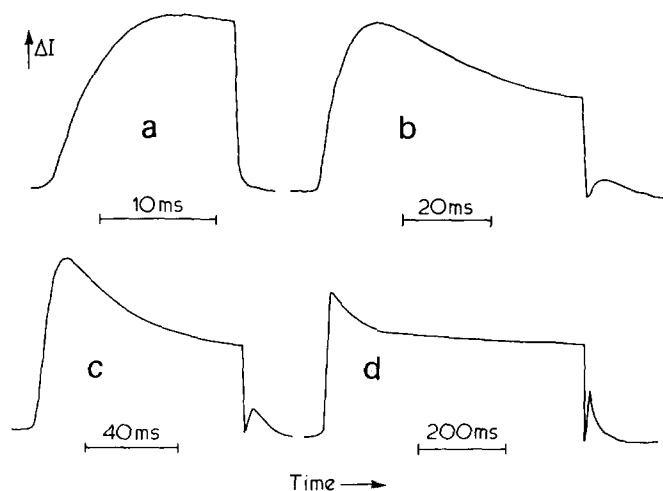


Figure 4 Quadratic Kerr-effect transients of PPG 1025 at 217K for different durations of applied electric field ($E \sim 4 \text{ V m}^{-1}$)

is allowed to attain equilibrium when an electric field is applied. This requirement was found to be essential for melt samples of poly(propylene glycol). If equilibrium conditions were not achieved prior to the step-removal of the electric field then the shapes of the optical decay transients exhibited gross departures from those obtained for the equilibrium case. If the optical transients can be regarded as a superposition of a fast negative birefringence component and a slower positive birefringence component (see below) then the decay relaxation times associated with these two processes are substantially modified by the failure to attain equilibrium in the presence of the electric field. This behaviour is demonstrated in Figure 4, which shows optical transient curves (quadratic detection) of PPG 1025 obtained by applying an electric field of constant magnitude but of variable duration. For this reason care was taken to ensure that the system reached equilibrium before the decay transient was initiated.

The unusual shape of the optical transient curves suggested that it might be possible to interpret the relaxation data using the equations derived by Benoit²⁸ for dipolar, polarizable molecules diffusing by small-angle steps. Benoit's equation for the rise and decay regimes of the optical transient are respectively,

$$\Delta n_E(t) = \Delta n_{eq} \left\{ 1 - \left[\frac{3}{2} \alpha \psi_1(t) + \left(\frac{\alpha}{2} - 1 \right) \psi_2(t) \right] \left[\alpha + 1 \right]^{-1} \right\}$$

and

$$\Delta n_0(t) = \Delta n_{eq} \psi_2(t) \quad (2)$$

where $\Delta n_E(t)$ is the transient optical birefringence at time t after the step-application of the electric field and $\Delta n_0(t)$ is the transient optical birefringence at time t after the step-removal of the electric field. Δn_{eq} is the equilibrium value of the optical birefringence ($\Delta n_E(t \rightarrow \infty) = \Delta n_0(t \rightarrow 0) = \Delta n_{eq}$). $\alpha = P/Q$ where $P = (\mu/kT)^2$ and $Q = (\Delta\alpha^0/kT)$ and μ and $\Delta\alpha^0$ are, respectively, the permanent dipole moment and the anisotropy of optical polarizability of the molecule. $\psi_1(t) = \exp(-2D_R t)$ and $\psi_2(t) = \exp(-6D_R t)$, where D_R is the molecular rotational diffusion constant. For the case in which $\alpha = 1/2$, equation 1 predicts that $\Delta n_E(t)$ increases to a maximum negative value and then slowly decreases to a smaller negative equilibrium value. This behaviour is similar

qualitatively to that observed experimentally for melt samples of poly(propylene glycol) (Figures 3 and 4). However, equation 2 predicts that $\Delta n_0(t)$ decays to zero as $t \rightarrow \infty$, without a change of sign, which is different from the optical decay curves obtained for PPG. The ratios of secondary to primary Kerr-effect decay times, $\tau_{k,d}^B/\tau_{k,d}^A$, for PPG 1025, PPG 2025 and PPG 4000 are approximately 20, 30 and 250, respectively, whereas the ratio of time constants associated with ψ_1 and ψ_2 has a fixed value of 3. It is concluded that the present Kerr-effect relaxation data for PPG cannot be interpreted using the above relationships (equations 1, 2) derived by Benoit for small-angle rotational diffusion. Consequently, the rise and decay regimes of the optical transient curves were analysed using two components: primary (A), associated with a 'fast' negative optical birefringence; and secondary (B), associated with a 'slow' positive optical birefringence. Figure 5 shows Kerr-effect data for PPG 2025 at 238 K presented as $\log_e [\Delta n_E(t) - \Delta n_{eq}]$ vs. t for the rise transient and $\log_e [\Delta n_0(t)]$ vs. t for the decay transient, plotted using values of $\Delta n_E(t)$ and $\Delta n_0(t)$ dominated by the secondary process. The data may be adequately described by a single-relaxation-time function. Subtraction of the secondary process from the total optical transient curve gave the net primary rise and decay processes.

Figures 6a, 6b and 6c show Kerr-effect rise and decay data of PPG 1025, PPG 2025 and PPG 4000, expressed as the equivalent frequency of maximum loss $f_m = (2\pi\tau)^{-1}$ plotted against reciprocal temperature. Each Figure shows dielectric and Kerr-effect data for both the primary (A) and the secondary (B) processes. Rise and decay optical transients for the primary process did not follow a single exponential time function and consequently these data were fitted to the empirical relationship of Williams and Watts³⁹ $\phi(t) = \exp[-(t/\tau_0)^\beta]$. The optimum value of β was approximately 0.7, a value typical for viscous liquids undergoing structural relaxation (α -process) just above the glass-transition temperature^{23,24,40,41}.

Figure 7 diagrammatically shows the relative frequency location of Kerr-effect and dielectric relaxation processes

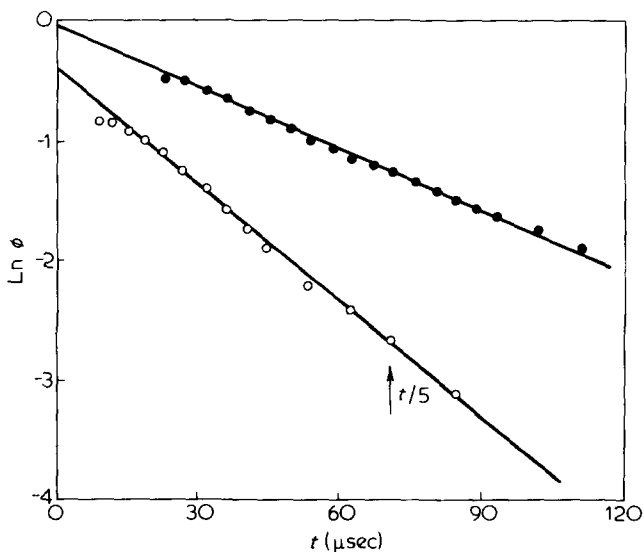


Figure 5 Kerr-effect transient data measured using linear detection for secondary (B) process of PPG 1025 at 238K ($E \sim 4 \text{ V m}^{-1}$). (O) rise function $\phi = \Delta n_E(t) - \Delta n_{eq}$, (●) decay function $\phi = \Delta n_0(t)$. Note that the data have not been normalized because no data is available at short times, due to convolution of relaxation processes A and B

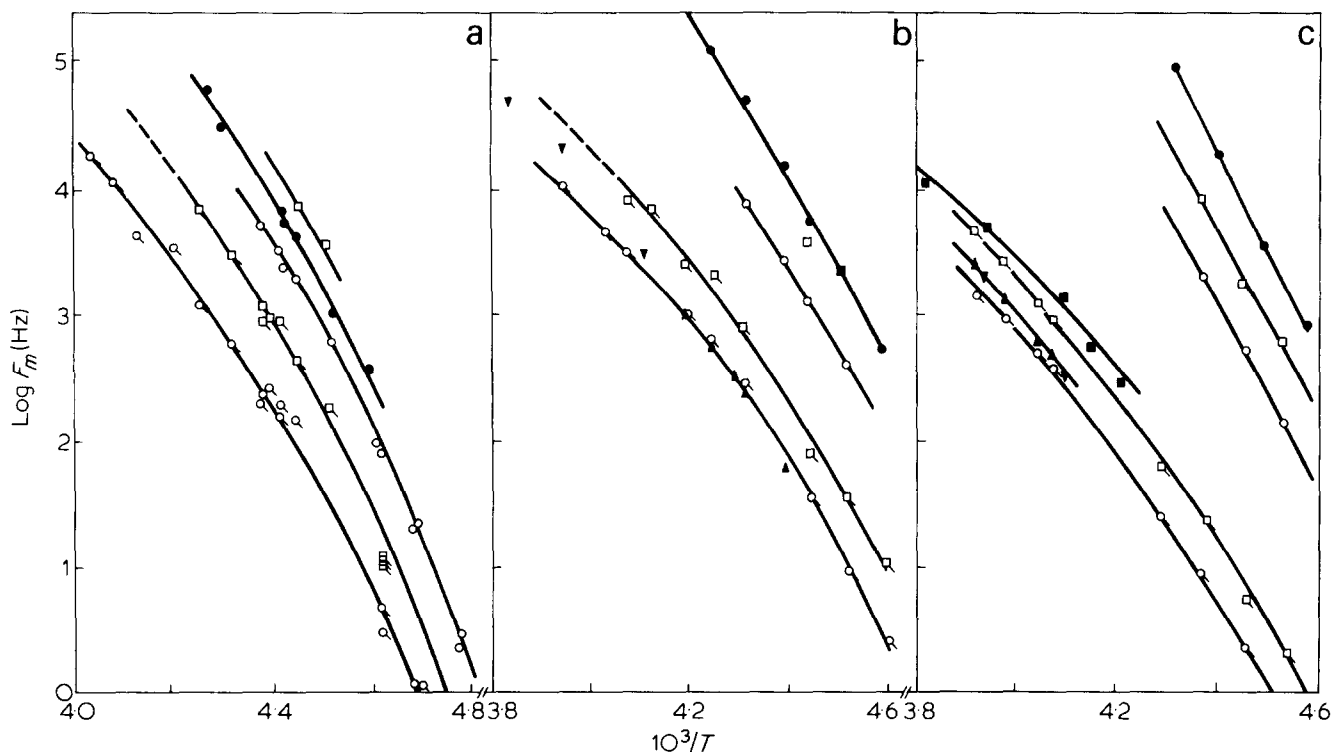


Figure 6a Relaxation data of PPG 1025. Primary (A) process: ● dielectric, ○ Kerr-rise, □ Kerr-decay. Secondary (B) process: ◊ Kerr-rise, ◊ Kerr-decay

Figure 6b Relaxation data of PPG 2025. Primary (A) process: ● dielectric data, ○ Kerr-rise, □ Kerr-decay. Secondary (B) process: ▲ dielectric, ▼ dielectric data of Baur and Stockmayer³⁵, ◊ Kerr-rise, ◊ Kerr-decay

Figure 6c Relaxation data of PPG 4000. Primary (A) process: ● dielectric, ○ Kerr-rise, □ Kerr decay. Secondary (B) process: ▲ dielectric, ▼ dielectric data of Baur and Stockmayer³⁵, ■ dielectric data of Alper et al.⁴¹, ◊ Kerr-rise, ◊ Kerr decay

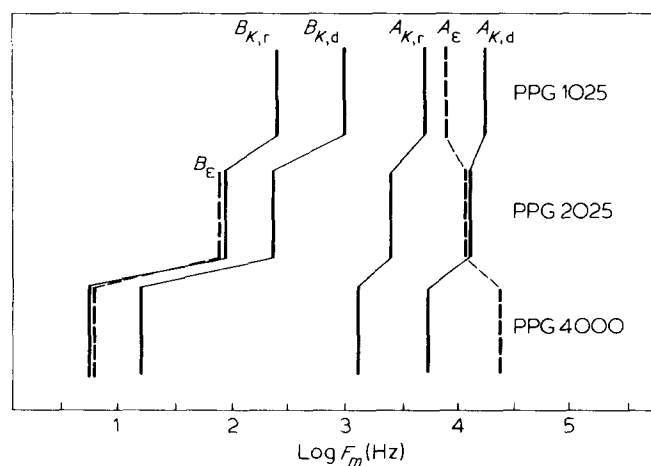


Figure 7 Frequency location of dielectric and Kerr-effect relaxation of the primary (A) and secondary (B) processes of poly(propylene glycol) at 227 K

for PPG 1025, PPG 2025 and PPG 4000 at 227 K. This diagram demonstrates the marked displacement to lower equivalent frequencies of the Kerr relaxation data for the primary (A) and the secondary (B) processes as the molecular weight is increased. In contrast, the frequency location of the maximum dielectric loss for the primary (A) process is displaced to higher frequencies with increasing molecular weight, a trend also observed by Baur and Stockmayer³⁵. Relaxation times of the Kerr-rise and Kerr-decay for the primary process are approximately a linear function of the molecular weight. Dielectric data for the secondary process of PPG 4000 has a similar frequency location and temperature dependence to that observed by Baur and Stockmayer³⁵ for a sample of

PPG of similar molecular weight. A comparison of the present dielectric relaxation data with that obtained by Alper *et al.*⁴¹, for the secondary (B) process for PPG 4000 (their P4000) revealed a discrepancy of a factor of approximately two in the position of the frequency of maximum loss.

For the secondary relaxation process the Kerr-effect rise times, $\tau_{K,r}$, are longer, by a factor of at least 2, than the corresponding Kerr-effect decay times, $\tau_{K,d}$, and the ratio of dielectric relaxation times to Kerr-effect decay times, $\tau_e/\tau_{K,d}$ is approximately equal to 3. Such relationships indicate that rotational diffusion is proceeding via small-angle steps³¹. However, this interpretation must be regarded as tentative, since the theory used to predict the above relationships is only strictly applicable to axially symmetric molecules undergoing free rotational diffusion³¹, and does not include the cross-correlation functions between the dipolar polarizable groups.

DISCUSSION

The recent experimental and theoretical work of De Gennes^{42,43}, Doi and Edwards⁴⁴, Klein⁴⁵ and others^{46,47} has led to the view that the diffusion of polymer molecules, in the bulk and in concentrated solution, may occur partly by 'reptation', a term first used by De Gennes⁴². The mechanism for reptation involves the curvilinear propagation of kink-like defects along a polymer chain confined to a virtual 'tube', the surface of which is defined by points of contact between the reptating chain and neighbouring chains. The relaxation times associated with 'reptation' and with 'tube' reorganization, and their dependence on molecular weight, have been studied by De Gennes^{42,43} and by Doi and

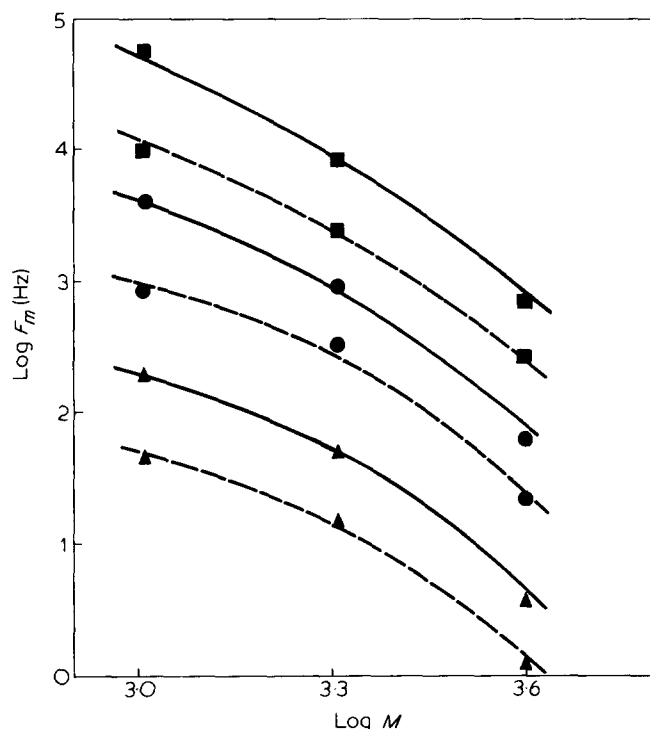


Figure 8 Molecular weight dependence of the secondary Kerr-effect relaxation processes of PPG. Rise data (---) and decay data (—) at \blacktriangle 222 K, \bullet 233 K, \blacksquare 244 K

Edwards⁴⁴ for similar model systems. De Gennes has considered the situation where a single, ideal polymeric chain is embedded in a fixed, three-dimensional polymeric gel and has obtained, (1) T_d (longest time) = $(Na)^2 \Delta / \pi$, ($\propto M^2$), for the time for equilibration of defects along the chain, and (2) $T_r = (Na)^3 / \pi^2 \bar{\rho} b^2 \Delta$, ($\propto M^3$), for the time taken for a complete conformational change or rearrangement of the virtual 'tube'. The model parameters are: a , the curvilinear interval between statistically independent 'monomer units' (in the absence of defects); b , the length of chain (stored length) associated with a single defect; Δ , the defect diffusion coefficient; and $\bar{\rho}$, the average number of defects per unit length of chain. If a polymer molecule possesses a cumulative permanent dipole moment along the longitudinal axis of the chain then T_r may be associated with a dielectric relaxation time³⁵. This is the case for poly(propylene glycol) polymerized to give a predominantly head-to-head structure, since the monomer dipole moment vector does not exactly bisect the C—O—C angle.

The recent theoretical work of Doi and Edwards⁴⁴, using the concept of a primitive chain to describe the motions of polymer molecules in the bulk, has demonstrated that time correlation functions which depend linearly on the Langevin equation for Brownian diffusion are the same as those derived for the Rouse chain model. This would be case for the diffusion of the centre of mass of the polymer chain. In the Rouse model the chain is permitted to reorientate at any point, whereas for the primitive chain of Doi and Edwards the terminal regions only are permitted to change their direction rapidly. An example of experimental evidence which would be expected to highlight this difference between these two models is provided by the decay of the incoherent, $S_{incoh}(k, t; s)$ and coherent, $S_{coh}(k, t)$ scattering factors. The molecular weight dependence of the characteristic decay rates for both of these quantities are predicted to be significantly different for the two models⁴⁴.

At the time of writing there have been few studies specifically designed to investigate 'reptation' in pure, low molecular weight polymeric systems. Klein⁴⁵ has measured the 'overall diffusion constant', \bar{D} , for narrow molecular weight fractions of deuterated polyethylene in a high molecular weight matrix of a molten polyethylene ($M \sim 1.6 \times 10^5$) at 449 K. Diffusion data obtained over the molecular weight range $M = 3.6 \times 10^3 - 2.3 \times 10^4$ were described by the simple relationship $\bar{D} = 0.2 M_w^{2.0} (\text{cm}^2 \text{s}^{-1})$ and support the model of 'reptation' proposed by De Gennes⁴². Kimmich and Schmauder⁴⁷ have used a fitting procedure to interpret n.m.r. relaxation data, obtained by Preissing⁴⁸ and Preissing and Noack⁴⁹ for bulk poly(ethylene oxide), according to the model for the 'reptation' of polymer molecules proposed by De Gennes⁴⁸.

Figure 7 demonstrates the effect of molecular weight on the frequency of maximum dielectric loss f_m for the A and B processes at 227 K. The location of the A process for PPG 4000 is displaced by approximately a half-decade to higher frequencies, relative to that observed for PPG 1025. After methylation of the terminal hydroxyl groups of PPG 2025 it was found that values of $\log f_m$, for the A process, were shifted to higher frequencies at any given temperature³⁵. These observations may be accounted for by the formation of hydrogen bonds between terminal hydroxyl groups and the oxygens of the ether groups. At any given time, a proportion of the ether groups will be involved in hydrogen bonding and their rate of diffusion is expected to be slower than that of 'free' unassociated ether groups and hydroxyl groups. Since the ratio of hydroxyl groups to ether groups varies inversely with molecular weight, the location of f_m for the primary (A) dielectric process would be expected to approach an upper limiting value provided that there were no other effects present which depended on molecular weight.

Figure 8 shows Kerr-effect data for the secondary (B) relaxation process of PPG presented as $\log f_m$ vs. $\log M$ for three different temperatures. The average gradient of the lines joining isothermal pairs of $\log f_m$ for PPG 1025 and PPG 2025 corresponded to a molecular weight dependence of $\tau \propto M^{-1.95 \pm 0.2}$ where the exponent was calculated using Kerr-effect decay times $\tau_{K,d}$. This compares favourably with the relationship, $\tau \propto M^{-2}$, predicted by De Gennes⁴² for a reptating chain. However, a similar analysis using isothermal pairs of $\log f_m$ for PPG 2025 and PPG 4000 yielded the relationship $\tau \propto M^{-3.7 \pm 0.2}$, indicating that the dependence of τ on molecular weight is changing rapidly as a function of molecular weight itself. In deriving these relationships we have used nominal molecular weights quoted by the supplier. The molecular weight dependence of the primary and secondary optical relaxation processes would be modified by the use of either the number-average, M_n , or weight-average, M_w , molecular weight and to an extent depending on the polydispersity. Thus, Alper *et al.*⁴¹ quote a number-average molecular weight of 3030 for their P4000. A comparison of relaxation data for the B process of PPG in the bulk with present theoretical predictions would be expected to be tenuous, since De Gennes has indicated that a separate and more difficult theoretical treatment is required to describe reptational diffusion in systems containing many mobile polymer chains. De Gennes' theory requires that the conformational behaviour of a polymer chain may be represented equivalently by a large number of statistically independent subunits. For the low molecular weight samples of PPG used in the present study, this requirement is probably not fulfilled.

The correlation between dielectric and Kerr-effect relaxa-

tion times, for the primary and secondary relaxation processes, indicates that these techniques are probing different aspects of, essentially, the same molecular motion. The dielectric relaxation of PPG depends mainly on the dipolar ether groups and terminal hydroxyl groups, whereas the corresponding Kerr-effect relaxation depends on the reorientational motions of all of the optically anisotropic sections of the polymer chain (e.g. $-\text{CH}(\text{CH}_3)\text{CH}_2-$ and $-\text{CH}_2\text{OCH}=\text{}$). Since the optical polarizability is a tensor, it follows that it is not essential that the polymer molecule possesses a head-to-tail repeat structure in order to observe a secondary Kerr-effect relaxation process. The magnitude and time-dependence of the secondary (B) dielectric relaxation process in PPG is expected to be dominated by cross-correlation terms, $\langle \mu_i(0) \cdot \mu_j(t) \rangle$; where μ_i and μ_j are contributions from the i th and j th structural units of the chain to the cumulative dipole moment. Similar time-dependent terms $\langle T_{ij}(t) \alpha_j^0 T_{ij}^{-1}(t) \rangle$, may be written for the cumulative optical polarizability tensor; where α_j^0 is the optical polarizability tensor associated with the j th structural unit of the chain and $T_{ij}(t)$ is the time-dependent transformation matrix required to express α_j^0 in the local coordinate system attached to the i th structural unit. In principle it should be possible to extend well established matrix algebra methods⁵⁰, used for calculating the equilibrium dipole moment and optical anisotropy of chain molecules, to evaluate a time-dependent stochastic model for the conformational behaviour of a polymer molecule bounded by a matrix of adjacent chains. In practice, it is probable that 'molecular dynamics' calculations will prove to be more tractable than a stochastic approach in the evaluation of different models for the rotational and translational diffusion of polymer molecules in the melt or in their concentrated solutions.

We note that transient electro-optical effects may arise from the presence of impurities (suspended or dissolved) or from electrostriction in the medium. We have no evidence that impurities contribute to the observed behaviour for the different polypropylene glycols studied here. With regard to electrostriction, dilation of the liquids in response to step-on fields was observed, and corresponded certainly to an increase in the number density of molecules in the inter-electrode space. If this density increase is isotropic in nature then no Kerr-effect is obtained. However, the electrostriction effect may be anisotropic, (i.e. the molecules are aligned partially during the electrostriction process) and this would lead to a Kerr-effect. Flow of the polymer liquid into the inter-electrode space, as a part of establishing the electrostriction equilibrium, would also lead to a Kerr-effect. The magnitude and importance of these effects are not readily estimated. Such effects may make a contribution to the behaviour we have described for polypropylene glycol liquids.

We also note that during the course of studies of the electro-optical properties of conducting liquids, we have observed transients which are similar in form to those for liquid PPG. For the conducting liquids it appears that electrode polarization leads to a substantial field gradient near to the electrodes with a corresponding diminution of the field in the bulk of the liquid – and hence to a transient lowering of the birefringence. We cannot rule out the possibility that a similar effect may make a contribution to the long-time transients for PPG.

ACKNOWLEDGEMENTS

M.S.B. and D.A.E. gratefully acknowledge financial assistance provided by the S.R.C. and the award of an equipment grant

from the S.R.C. The Computer Unit of the University College of Wales, Aberystwyth is thanked for the provision of computing facilities, and we thank Prof. A. J. Barlow (University of Glasgow) for the provision of a sample of PPG 4000.

REFERENCES

- 1 McCrum, N. G., Read, B. E. and Williams, G. 'Anelastic and Dielectric Effects in Polymeric Solids', Wiley, London, New York, 1967
- 2 Hedvig, P. 'Dielectric Spectroscopy of Polymers', Adam Hilger, Bristol, 1977
- 3 Karasz, F. E. (Ed.) 'Dielectric Properties of Polymers', Plenum Press, New York, 1972
- 4 Wada, Y. in 'Dielectric and Related Molecular Processes', (Ed. M. Davies) Spec. Period. Report, Chem. Soc., London, Vol. 3, 1977, p 143
- 5 Ferry, J. D. 'Viscoelastic Properties of Polymers', 2nd Edn., Wiley, New York, 1970
- 6 Slichter, W. P. in 'NMR, Basic Principles and Progress', Vol 4, 'Natural and Synthetic High Polymers', Springer Verlag, Berlin, 1971, p 209
- 7 Connor, T. M. *ibid*, p 247
- 8 Schaefer, J., Stejskal, E. O. and Buchdahl, R. *Macromolecules*, 1977, **10**, 384
- 9 Allen, G. and Higgins, J. S. *Rep. Progr. Phys.* 1973, **36**, 1073
- 10 Block, H. and North, A. M. *Adv. Mol. Relaxation Processes* 1970, **1**, 309
- 11 Bovey, F. A., Schilling, F. C., Kwei, T. K. and Frisch, H. L. *Macromolecules* 1977, **10**, 757
- 12 Cais, R. E. and Bovey, F. A. *Macromolecules* 1977, **10**, 169, 752, 757
- 13 Berne, B. J. and Pecora, R. 'Dynamic Light Scattering', Wiley-Interscience, New York, 1976
- 14 Valeur, B. and Monnerie, L. *J. Polym. Sci. Polym. Phys. Edn.* 1976, **14**, 11, 29
- 15 Williams, G. 'Advances in Polymer Science', 1978 in press
- 16 Williams, G. and Crossley, J. *Ann. Rep. A, Chem. Soc., London* 1978, in press
- 17 Stockmayer, W. H. *J. Phys. (Paris) Colloq.* 1971, **5**, 255
- 18 Stockmayer, W. H. *Makromol. Chem.* 1973, **8**, 379
- 19 Stockmayer, W. H. *Pure Appl. Chem.* 1967, **15**, 247
- 20 Curtiss, C. F., Bird, R. B. and Hassager, O. *Adv. Chem. Phys.* 1976, **35**, 31
- 21 Bird, R. B., Armstrong, R. C. and Hassager, O. 'Dynamics of Polymeric Liquids', Vol. 1, 'Fluid Mechanics', Wiley, New York, 1976
- 22 Bird, R. B., Hassager, O., Armstrong, R. C. and Curtiss, C. F. 'Dynamics of Polymeric Liquids', Vol 2, Wiley, New York, 1976
- 23 Beevers, M. S., Crossley, J., Carrington, D. C. and Williams, G. *J. Chem. Soc. Faraday Symp.* No. 11, 1976, 38
- 24 Beevers, M. S., Crossley, J., Garrington, D. C. and Williams, G. *J. Chem. Soc. Faraday Trans. II*, 1977, **73**, 458
- 25 Berne, B. J. in 'Physical Chemistry, An Advanced Treatise', Vol. VIII B, 'The Liquid State', (Eds. H. Eyring, W. Jost and D. Henerson) Academic Press, New York, 1971
- 26 Williams, G. *Chem. Rev.* 1972, **72**, 55
- 27 Williams, G. *Chem. Soc. Rev.* 1978, **7**, 89
- 28 Benoit, H. *Ann. Phys.* 1951, **6**, 561
- 29 O'Konski, C. T. and Zimm, B. H. *Science* 1950, **111**, 113
- 30 Fredericq, E. and Houssier, C. 'Electric Dichroism and Electrical Birefringence', Oxford University Press, London, 1974
- 31 Beevers, M. S., Crossley, J., Garrington, D. C. and Williams, G. *J. Chem. Soc., Faraday Trans. II*, 1976, **72**, 1482
- 32 Crossley, J. and Williams, G. *J. Chem. Soc., Faraday Trans. II*, 1977, **73**, 1651, 1906
- 33 Crossley, J., Elliott, D. A. and Williams, G. *J. Chem. Soc., Faraday Trans. II*, 1978, **75**, 88
- 34 Beevers, M. S., Elliott, D. A. and Williams, G. *Polym. Lett.* 1979 in press
- 35 Baur, M. and Stockmayer, W. H. *J. Chem. Phys.* 1965, **43**, 4319
- 36 Le Fèvre, R. J. W. and Solomons, S. C. *Aust. J. Chem.* 1968, **21**, 1703
- 37 Le Fèvre, R. J. W. and Sundaram, K. M. S. *J. Chem. Soc. Perkin II*, 1972, 2325

- 38 Aroney, M. J., Le Fèvre, R. J. W. and Saxby, J. J. *Chem. Soc.* 1962, **563**, 2886
- 39 Williams, G., Watts, D. C., Dev, S. B. and North, A. M. *Trans. Faraday Soc.* 1971, **67**, 1323
- 40 Williams, G., Cook, M. and Hains, P. J. *J. Chem. Soc. Faraday Trans. II* 1972, **68**, 1045
- 41 Alper, T., Barlow, A. J. and Gray, R. W. *Polymer* 1976, **17**, 665
- 42 De Gennes, P. G. *J. Chem. Phys.* 1971, **55**, 572
- 43 De Gennes, P. G. *Macromolecules* 1976, **9**, 587
- 44 Doi, M. and Edwards, S. F. *J. Chem. Soc. Faraday Trans II*, 1978, **74**, 1789, 1802, 1818
- 45 Klein, J. *Nature* 1978, **271**, 143
- 46 Kimmich, R. *Polymer* 1977, **18**, 233
- 47 Kimmich, R. and Schmauder, Kh. *Polymer* 1977, **18**, 239
- 48 Preissing, G. Thesis, Stuttgart, 1973
- 49 Preissing, G. and Noack, F. *Prog. Colloid Polym. Sci.* 1975, **57**, 216
- 50 Flory, P. J. 'Statistical Mechanics of Chains Molecules', Interscience, New York, 1969